Symptomatic malaria enhances protection from reinfection with homologous *Plasmodium falciparum* parasites

Christine F. Markwalter,[1#] Jens E. V. Petersen,[2#] Erica E. Zeno,[2,3] Kelsey M. Sumner,[2,3] Elizabeth Freedman,[2] Judith N. Mangeni,[4] Lucy Abel,[5] Andrew A. Obala,[6] Wendy Prudhomme-O'Meara,[1,2,4] Steve M. Taylor[1,2,3]*

[1] Duke Global Health Institute, Duke University, Durham NC USA
[2] Division of Infectious Diseases, School of Medicine, Duke University, Durham NC USA
[3] Department of Epidemiology, Gillings School of Global Public Health, University of North Carolina, Chapel Hill NC USA
[4] School of Public Health, College of Health Sciences, Moi University, Eldoret, Kenya
[5] Academic Model Providing Access to Healthcare, Moi Teaching and Referral Hospital, Eldoret Kenya
[6] School of Medicine, College of Health Sciences, Moi University, Eldoret Kenya
[#] Contributed equally
* Corresponding author:
Steve M Taylor
steve.taylor@duke.edu

ABSTRACT

A signature remains elusive of naturally-acquired immunity against *Plasmodium falciparum.* We identified *P. falciparum* in a 14-month cohort of 239 people in Kenya, genotyped at immunogenic parasite targets expressed in the pre-erythrocytic (circumsporozoite protein, CSP) and blood (apical membrane antigen 1, AMA-1) stages, and classified into epitope type based on variants in the DV10, Th2R, and Th3R epitopes in CSP and the c1L region of AMA-1. Compared to asymptomatic index infections, symptomatic malaria was associated with a reduced reinfection by parasites bearing homologous CSP-Th2R (adjusted hazard ratio [aHR]:0.63; 95% CI:0.45–0.89; p=0.008) CSP-Th3R (aHR:0.71; 95% CI:0.52–0.97; p=0.033), and AMA-1 c1L (aHR:0.63; 95% CI:0.43–0.94; p=0.022) epitope types. The association of symptomatic malaria with reduced risk of homologous reinfection was strongest for rare epitope types. Symptomatic malaria more effectively promotes functional immune responses. The phenotype represents a legible molecular epidemiologic signature of naturally-acquired immunity by which to identify new antigen targets.

INTRODUCTION

Malaria kills over 400,000 people annually[1] owing in part to the slow development of incomplete, naturally-acquired immunity (NAI). NAI provides reliable protection against severe malaria after a few infections[2] but does not wholly prevent symptomatic malaria, owing in part to short-lived immune responses and to *P. falciparum* antigenic variation that collectively limit the effectiveness of antibodies.[3-7] The mechanisms and targets of functional responses remain incompletely understood, complicating efforts to recapitulate these responses for the purposes of vaccine development. The rational design of the next generation of *P. falciparum* vaccines that are informed by mechanistic insights furnished by models of NAI would be enhanced by the identification of robust phenotypes of acquired protection in naturally-exposed populations. Similar to other pathogens, a hallmark of functional protection against malaria is the delayed acquisition or decreased risk of infection when exposed to homologous parasites.[8] The phenotype of homologous protection against either infection or severity has been observed using a variety of approaches including challenge studies of a radiation-attenuated *Plasmodium falciparum* sporozoite vaccine[9,10] and of *P. vivax* used as neurosyphilis therapy,[11] as well as in field studies of monovalent vaccines targeting *P. falciparum* apical membrane antigen 1 (AMA-1)[12] and circumsporozoite protein (CSP).[7] Detecting this signature of functional protection is a challenge in observational field studies because the frequency of infections renders such studies operationally complex, and the genetic diversity of parasites and multiplicity of infections complicates strain-typing methods. Capturing homologous reinfection events and measuring associations with host and parasite factors in a natural setting can provide insights into the process by which anti-parasite immune memory is inscribed.

Herein, we explore how exposure to diverse sequence types in a high-transmission setting influences the time to reinfection with *P. falciparum*. We focused on immunogenic segments of antigens expressed in the pre-erythrocytic (CSP) and the blood (AMA-1) stages in our previously-published *P. falciparum pfcsp* and *pfama1* sequences collected in our longitudinal cohort of 239 people who suffered 902 asymptomatic and 137 symptomatic *P. falciparum* infections over 14 months of observation.[13] Given that symptomatic malaria, which is associated with overexpression of pro-inflammatory cytokines IFN-γ, TNF, and IL-1β,[14] is associated with the subsequent development of more robust functional immune response[15] similar to other pathogens including SARS-CoV2,[16] we explored if symptomaticity influenced the risk of reinfection with parasites bearing homologous CSP and AMA-1 types. We hypothesized that, compared to asymptomatic infections, symptomatic malaria would prolong the time to reinfection with parasites bearing homologous CSP and AMA-1 types.

RESULTS

Analytic population and risk of reinfection

As previously reported, between June 2017 and July 2018 in Webuye, Kenya, we collected 902 asymptomatic and 137 symptomatic *P. falciparum* infections; from these, amplification and sequencing was successful for *pfcsp* in 861 samples and for *pfama* in 724 samples.[13] For each participant, we defined the start and end of infection episode, each composed of a single or of multiple contiguous *P. falciparum* positive samples (**Figure 1**) and then calculated the time to reinfection as the time from the end of one index episode to the start of the next. We excluded from analysis index episodes for which time to reinfection was less than or equal to 60 days for 3 reasons: 1) our analysis was motivated to detect a signature of functional immunity which would be unlikely to manifest immediately; 2) to minimize the risk of bias introduced by either recrudescent infections after symptomatic infection or falsely-negative haplotype capture after asymptomatic infection; and 3) our sampling scheme of monthly active surveillance for asymptomatic infections, when combined with the definition of an end of infection as the absence of the parasite or type in the next sampling, resulted in an effective floor of 60 days for reinfection following an asymptomatic infection that was not present for passively-detected symptomatic infections. These excluded index episodes were more likely to be symptomatic (**Supplemental Table**) and to occur in the high transmission season, but were otherwise similar to the non-excluded infections. Therefore, we computed the time to reinfection following 275 asymptomatic and 69 symptomatic infection episodes that composed the analytic dataset. Between asymptomatic and symptomatic infections, we observed differences in transmission season, multiplicity of infection (MOI), parasite density, and read coverage. However, read coverage was high in both the asymptomatic and symptomatic groups, so it is unlikely that read coverage is driving MOI (**Table 1**).

We first compared between symptomatic and asymptomatic episodes the risk of reinfection among all participants irrespective of parasite sequence type. The median time to reinfection was 126 days (95% CI 119-150), and the probability of remaining free of reinfection within 1 year of index exposure was 0.07 (95% CI 0.04-0.13) (**Figure 2A**). In a multivariate mixed effects Cox proportional hazards model, compared to asymptomatic infections, the presence of symptoms during the index infection was not associated with the hazard of reinfection (aHR 1.04; 95% CI 0.74-1.46) (**Figure 2B**).

P. falciparum CSP and AMA-1 amino acid diversity

To enable an analysis of reinfection with homologous parasites, we next assessed the parasite genotypes within these infections, in which, as previously reported,[13] we observed 155 unique *pfcsp* and 209 unique *pfama* nucleotide sequences. These encoded 145 unique CSP amino acid (AA) sequences with missense substitutions, which resulted from variance in 39 of the 95 AA positions captured by sequencing (**Figure 3A**), and 203 unique AMA-1 AA sequences, which resulted from variance in 50 of the 99 AA positions captured by sequencing (**Figure 3C**).

In order to reduce these highly diverse antigen segments into broader, biologically relevant groups and preserve statistical power, we identified the (1) most informative variable AA positions that (2) occurred in immunologically-relevant antigen segments. To focus on AA positions that would be most informative, we utilized a Random Forest approach to rank the ability of the variant AA positions to correctly predict the full nucleotide sequences (**Figure 3B**). The most informative AAs were clustered in three main variable areas of our CSP sequence: in the linker to the NANP repeat region harboring the DV10 epitiope, the Th2R CD4+ T-cell epitope,[17] and the Th3R CD8+ T-cell epitope.[18] For AMA-1 the most informative among the 50

variant positions AA positions were distributed across four apparent clusters, one of which included the immunogenic c1L domain[19] (**Figure 3D**).

Next, we classified each parasite in each infection based on the four most predictive AA positions in the i) CSP DV10 epitope, ii) CSP Th2R epitope, iii) CSP Th3R epitope, and iv) AMA-1 c1L domain (hereafter CSP-DV10, CSP-Th2R, CSP-Th3R, or AMA-1 c1L epitope types, respectively). We observed 8 unique CSP-DV10 epitope types, 27 unique CSP-Th2R epitope types, 14 unique CSP-Th3R epitope types, and 20 unique AMA-1 c1L types. Within individual infections, the multiplicity of infection (MOI) expressed by nucleotide sequence was very closely correlated when computed based on the CSP-Th2R epitope type (ratio 1:0.95) and less so when computed by CSP DV10 (ratio 1:0.4), CSP-Th3R epitope type (ratio 1:0.6), or AMA-1 c1L type (ratio 1:0.7) (**Supplemental Figure 1**). The CSP DV10 epitope had a notably lower level of epitope type diversity relative to CSP-Th2R, CSP-Th3R, and AMA-1 c1L, with 73% (2521/3443) of the *pfcsp* haplotype occurrences detected across 861 samples coding for the major epitope type. Subsequent analyses and results for the CSP-DV10 epitope are described in the Supplemental Results.

Risk of reinfection with homologous CSP or AMA-1 parasites
We next investigated the risk of reinfection by homologous parasites defined by these epitope types. To do so, we partitioned *P. falciparum* infections based on the presence of specific CSP-Th2R, CSP-Th3R, and AMA-1 c1L epitope types; as a result, each participant could harbor multiple concurrent type-defined episodes with varying origin and end dates (**Figure 1**). By this classification, we observed 2174 CSP-Th2R, 1462 CSP-Th3R, and 1367 AMA-1 c1L type infection episodes, and the time to homologous reinfection was then calculated as the time between the end of a specific type-defined episode to the beginning of the next type-defined episode harboring the same type. The prior exclusion of index infections for which time to reinfection was less than or equal to 60 days did not result in systematic exclusion of specific epitope types (**Supplemental Figure 2**).

Using these epitope classifications of parasites, the probability of homologous reinfection within a year was 0.46 (95% CI 0.43 - 0.48) when classified by CSP-Th2R, 0.55 (95% CI 0.52 - 0.59) by CSP-Th3R, and 0.44 (95% CI 0.40-0.47) by AMA-1 c1L (**Supplemental Figure 3**). There were no differences between these risks of reinfection observed for homologous parasites and those expected for random parasite types for those classified by CSP-Th2R epitope (median Chisq 0.518, median p 0.472 log lank test), the CSP-Th3R epitope (Chisq 0.320, p 0.571 log-rank test), or AMA-1 c1L (Chisq 0.249, p 0.618 log-rank test) (**Supplemental Figure 3**). This suggests that the risk of reinfection observed for homologous parasites was not different from that expected for a heterologous parasite across both symptomatic and asymptomatic index cases.

Risk of homologous reinfection in symptomatic and asymptomatic infections
Given the rationale that the presence of symptoms during an index infection reflects the presence of immune responses to the parasite, we next compared the risk of homologous reinfection between asymptomatic and symptomatic index cases. When classified by CSP-Th2R epitope type, the probability of reinfection with a homologous parasite in 1 year was higher in asymptomatic (0.48, 95% CI 0.44 – 0.51) than in symptomatic (0.32, 95% CI 0.25 – 0.39) index cases (**Figure 4**). In a multivariate mixed effects Cox model, compared to asymptomatic index episodes, the presence of symptoms during the index episode was associated with a significantly reduced risk of reinfection with parasite bearing a homologous CSP-Th2R type (adjusted hazard ratio (aHR) 0.63; 95% CI 0.45 – 0.89; p=0.008) (**Figure 4**). Similarly, the presence of symptoms was also associated with a decreased hazard of reinfection with

parasites bearing homologous CSP-Th3R types (aHR 0.71; 95% CI 0.52 – 0.97; p=0.033) and homologous AMA-1 c1L types (aHR 0.63; 95% CI 0.43 – 0.94; p = 0.022, **Figure 4**). The inclusion of MOI as a co-variate did not significantly impact these results for CSP-Th2R and CSP-Th3R epitopes but slightly decreased the hazard of homologous reinfection defined by AMA-1 c1L epitope types (**Supplemental Table 2**).

We then performed this comparison in randomized datasets, in which there were no consistent differences between symptomatic and asymptomatic index episodes of the risk of reinfection with homologous types defined by CSP-Th2R (log-rank (median) chisq 0.822, p 0.364), CSP-Th3R (chisq 0.495, p 0.481) or AMA-1 c1L (chisq 3.08, p 0.079), nor any association in Cox proportional hazard models between symptoms and time to reinfection (**Supplemental Figure 4**). These observations indicate that symptomatic infections are associated with a reduced risk of reinfection with parasites bearing homologous CSP or AMA-1 epitope types.

To support these findings, we also directly compared the risk reinfection with parasites bearing homologous epitope types and random epitope types after symptomatic index episodes and separately after asymptomatic index episodes (**Supplemental Figure 3**). We observed no difference in risk of homologous and random reinfection after asymptomatic index cases for any of the CSP or AMA-1 epitope types. However, the risk of homologous reinfection was lower than the risk of random infection after a symptomatic index case when classified by CSP-Th2R epitope types (log-rank median chisq 8.945, p = 0.0028). Similar trends, though not reaching statistical significance, were observed for CSP-Th3R (log-rank median chisq 2.793 p = 0.0947) and AMA-1 c1L (log-rank median chisq 2.542, p = 0.111).

An ensemble analysis of CSP-Th2R and CSP-Th3R is presented in the Supplemental Results.

Epitope type prevalence and risk of reinfection following symptomatic infection
We next investigated if delayed time to reinfection by homologous parasites following symptomatic infection was modified by the population prevalence of epitope type. To do so, we categorized the epitope types of each target into common, middling, and rare on the basis of the parasite population prevalence of the type and computed Cox proportional hazard models within each prevalence stratum. Epitopes were assigned to categories for each target to achieve approximately equal population frequency of each category (**Figure 5**). To varying degrees, we observed reduced hazards of homologous reinfection for each epitope type within each prevalence stratum, with the lowest hazards for homologous reinfection associated with symptomatic malaria observed for the rare CSP-Th2R (aHR 0.35, 95% CI 0.16 – 0.77, p=0.010) and AMA-1 c1L (aHR 0.23, 95% CI 0.08-0.68, p = 0.008) epitope types. There was moderate support for effect modification by epitope type frequency for models of both the CSP-Th2R (p=0.096 by log likelihood test) and AMA-1 c1L (p = 0.055) epitope types. These observations suggest that epitope type rarity within a parasite population modifies the effect of symptoms on the risk of homologous reinfection, in that symptomatic malaria more strongly reduces the risk of homologous reinfection for the rarest epitope types.

DISCUSSION

In this longitudinal cohort study with 14 months of follow-up in a high transmission setting in western Kenya, we investigated factors associated with the time to reinfection with malaria parasites bearing homologous CSP and AMA-1 sequences. We observed that, compared to asymptomatic infections, symptomatic malaria was associated with a reduced risk of reinfection by parasites bearing identical epitope types. Additionally, this increased protection from homologous reinfection that was associated with symptomatic malaria was observed across the full range of diverse CSP-Th2R, CSP-Th3R, and AMA-1 c1L types but was greatest for the rarest types. Given that delay in reinfection with homologous parasites is a signature of acquired functional immunity, these observations suggest that, compared to asymptomatic infections that are common in high-transmission settings, symptomatic infections more effectively inscribe anti-parasite immunity to build protection against malaria.

Our observation that the presence of symptoms is associated with a decreased risk of reinfection with parasites bearing homologous epitope types is consistent with enhanced engagement of the immune system during symptomatic infections. Our CSP types were defined by polymorphic residues in the known CD4[+16] and CD8^{+} T-cell[17] epitopes in the C-terminal domain, suggesting that T-cell responses are primed more effectively by symptomatic infections. T-cells participate directly and indirectly in functional immunity to malaria (reviewed in [20]), particularly directed towards the pre-erythrocytic stages of the parasites that express CSP. Recognition of these CSP epitopes by CD8[+21] or CD4[+22] T-cells has been associated with protection from malaria, although, notably, we did not observe overall protection from reinfection with homologous compared to random parasites (**Supplemental Figure 3**), suggesting that these functional responses to CSP epitopes are either promoted during symptomatic malaria or attenuated during an asymptomatic infection. Similarly, AMA-1 types were defined on residues comprising the c1L domain that encode the main targets of naturally-acquired anti-AMA-1 immunity,[19,23] supporting the notion that symptomaticity reflects the development of functional immunity. Consistent with this interpretation, in a cohort of Malian children,[15] febrile malaria resulted in the upregulation of multiple markers of adaptive immunity, including T-cell stimulation, opsonic and non-opsonic phagocytosis, and antigen processing. Our findings extend these observations to suggest that such immune effectors are strain-specific and ineffectively promoted by asymptomatic infections.

We observed that the risk of homologous reinfection was reduced following symptomatic infections across a diversity of CSP-Th2R, CSP-Th3R, and AMA-1 c1L types with widely varying population frequencies (**Figure 5**). The otherwise broad protection following symptomatic infection suggests that this phenomenon is not a biological consequence of specific sequence types or an epidemiologic artifact driven only by rare epitopes which are necessarily unlikely to recur. Interestingly, though risk reductions were similar across prevalence categories for parasites defined by CSP-Th3R type, we observed modification of this effect by the prevalences of CSP-Th2R and AMA-1 c1L epitope types, with a greater protection following symptomatic infection among the rarest types than the most common types. This suggests that the rarity of these epitope types may be a consequence of the protection conferred by symptomatic infections harboring them, and highlights a mechanism by which anti-parasite immunity shapes parasite diversity.

Several facts support the notion that the observed delay in homologous reinfection following symptomatic malaria represents a legible signature of functional anti-parasite immunity. Firstly, a delayed time-to-reinfection with a homologous pathogen strain is a common phenotype of functional immunity. Secondly, this delay in time-to-reinfection was observed when parasites were classified on the basis of known targets in CSP[17,18] and AMA-1[19,24] of functional responses

6

that have been measured and correlated with protection in a wide variety of approaches. Thirdly, the effect was observed across a diverse range of sequences and epitope type prevalences, indicating that it was not artifactually driven by specific over-represented epitopes. Additionally, and in contrast, the delay was not present when comparing time-to-reinfection with random epitope types (**Supplemental Figure 4**), indicating that the effect was specific to parasites harboring an exact epitope match and not an effect generalizable to alternate epitopes of similar population prevalence. Further, when the time to reinfection with parasites bearing homologous epitope types was directly compared to time to random reinfection, homologous reinfection was delayed relative to random reinfection only after symptomatic exposure (**Supplemental Figure 3**). Finally, this effect was not present when analyzed agnostic to parasite genotype (**Figure 2**), reflecting the importance of CSP and AMA-1 epitope type. Though this phenomenon is not easily measurable in most study designs, future longitudinal molecular epidemiologic studies could screen a wide variety of known and putative parasite antigens and correlate variants with the degree of delay in reinfection following a symptomatic episode as an approach to identifying promising targets of natural immunity.

It is notable that this phenomenon was observed for parasites classified by sequences of antigens expressed during both the pre-erythrocytic and the blood stage. Given that AMA-1 is expressed during the blood stage, the rationale is straightforward for symptomaticity during the blood stage to reflect enhancement of functional immunity directed against AMA-1. However, how might symptomaticity during the blood stage mediate functional immunity to variants of the CSP antigen that is expressed during the pre-erythrocytic stage? CSP is expressed on sporozoites and during the liver stage but not during the blood stage, and the typical delay between release from the liver and onset of symptoms of at least 4-8 days (or longer in semi-immune individuals) suggests CSP should no longer be present and eliciting responses. One potential explanation is persistence of CSP in exo-erythrocytic parasite forms and antigen-presenting cells, which can be found in the skin, liver, and lungs for an undetermined period of time.[25] Alternatively, given their critical role in pre-erythrocytic immunity,[26,27] effector CD8+ T-cells primed by CSP exposure may be converted more efficiently by the mechanisms which produce symptoms into memory CD8+ cells with the ability to rapidly confer pre-erythrocytic protection on re-exposure.[28] Finally, symptomaticity may cause or result from processes that influence regulatory T-cells, which have cryptic roles in adaptive immunity to malaria but are generally thought to modulate inflammation to parasitemia and acquisition of functional immunity.[29]

Two other observations are notable. First, the degree of protection against homologous reinfection associated with symptomatic infection was fairly consistent across classifications by DV10 (aHR 0.75), CSP-Th2R (aHR 0.63), CSP-Th3R (aHR 0.71), combined CSP-Th2R/Th3R (aHR 0.56), and AMA-1 c1L (aHR 0.63) epitope types. This is despite the varied effector mechanisms that are associated with each epitope, including recognition by B-cells, CD4+[17] or CD8+[18] T-cells, and by polyclonal sera.[19] This shared degree of protection suggests that symptomaticity may promote the acquisition of effective immunity to similar degrees across different effector mechanisms. Secondly, despite the vast *pfcsp* sequence diversity, the 155 unique *pfcsp* nucleotide haplotypes reduced to just 27 CSP-Th2R types with little loss in within-host diversity: within individuals, the observed number of CSP-Th2R epitope types was correlated nearly one-to-one with the number of unique *pfcsp* haplotypes, demonstrating a low level of redundant or silent nucleotide substitutions at the Th2R epitope. By contrast, significant loss of within-host diversity was observed when *pfcsp* sequences were classified by CSP-DV10 and CSP-Th3R epitopes, which reduced to 8 and 14 types, respectively (**Supplemental Figure 1**). This suggests that, within polyclonal infections, amino acid diversity of CSP is maximized at the Th2R epitope.

7

This study has some limitations. Precisely defining the start and end of infections is challenging. We mitigated this challenge by using the longitudinal study design and classifying the beginning and end of infections based on prior and subsequent samples being *P. falciparum*-negative to avoid misclassifying persistent infections. Additionally, symptomatic infections were necessarily treated upon diagnosis, which could bias comparisons with asymptomatic infections which ended without treatment. However, we did not observe a difference in risk of overall reinfection between symptomatic and asymptomatic cases (**Figure 2**), nor was there a difference in risk of reinfection with random epitope types (**Supplemental Figure 4**). Finally, our genotyping approach is subject to false discovery. This was mitigated by the application of stringent read- and haplotype-quality filtering.

In our longitudinal molecular epidemiologic study, compared to asymptomatic *P. falciparum* infections, symptomatic malaria was associated with an increased time to reinfection by parasites harboring homologous CSP and AMA-1 epitope types. The fact that these epitope types were defined by variant residues in known immunogenic regions supports the notion that a differential time-to-reinfection with homologous parasite strains between asymptomatic infection and symptomatic malaria represents a legible signature of functional immunity to *P. falciparum*. Future studies can adapt this framework to identify putative targets of naturally-acquired immunity in re-infection cohorts and identify additional parasitologic, clinical, or host factors that modify the process by which anti-disease immunity is inscribed.

METHODS

Inclusion and ethics statement

Written informed consent was provided by all adults and by parents or legal guardians for individuals under 18 years of age. Additional verbal assent was given by individuals between 8 and 18 years of age. The study was approved by the ethical review boards of Moi University (2017/36) and Duke University (Pro00082000).

Study design and sampling

The longitudinal cohort consisting of participants in three villages in Western Kenya has been described previously.[13,30] In brief, all household members over 1 year of age were offered enrollment, and demographic data was collected for each participant. Dried blood spot (DBS) samples were collected from participants every month and any time a participant experienced symptoms associated with malaria, when they additionally were tested for malaria with a rapid diagnostic test and treated if positive with Artemether-Lumefantrine. We analyzed parasite gene sequences that have been previously reported.[13,31] Briefly, *P. falciparum* was detected in genomic DNA isolated from all DBS using a real-time PCR assay,[32] variant targets in the genes encoding the apical membrane antigen-1 (*pfama1*) protein and the circumsporozoite protein (*pfcsp*) were amplified, these were sequenced on Illumina MiSeq, and sequencing reads were analyzed and haplotypes filtered as described previously.[13] The *pfama* and *pfcsp* gene fragments were translated into protein sequences. Seven CSP and three AMA-1 nucleotide sequences containing stop-codons were removed. Amino acid sequence logos were made across all the sequences of either CSP or AMA-1 based on the probability of amino acid residues at each position.

Random forest models

Random forest algorithms were generated to predict the nucleotide sequence based on all the variant amino acid positions. The number of amino acid positions to try per node split (mtry) was first evaluated using the TuneRF function where random forest models of 100 trees were created with varying mtrys on the CSP sequences. A final mtry of 10 was selected as this was the first mtry that resulted in on out-of-bag (OOB) error rate below 0.1. Each final random forest model contained 2000 trees, and the OOB error rate was evaluated. The mean decrease accuracy for each amino acid position was used as a measure of the importance of each position.

Exposure classifications

A sample was defined as an asymptomatic malaria case when positive for *P. falciparum* by qPCR in the absence of symptoms. A sample was defined as a symptomatic malaria case when positive for *P. falciparum* by rapid diagnostic test (RDT) and qPCR in the presence of a symptom consistent with malaria (aches, chills, congestion, cough, diarrhea, fever, or vomiting) during a sick visit.

Samples from each participant were classified based on the result of *P. falciparum* qPCR for the purpose of defining episodes of *P. falciparum* infection (**Figure 1**). For successive *P. falciparum* positive samples, the first positive sample was classified as the start of an infection episode, and the last positive sample before a negative sample was classified as the end of the infection episode. Symptomatic infections were classified as the end of an episode, since they were treated. All infections within 14 days of treatment were excluded from the dataset owing to the possibility of residual detectability following effective treatment. These samples at the end of an episode were treated as index cases, and time to reinfection was then calculated as the time between index case and the next *P. falciparum* positive sample. Index cases not followed by a *P. falciparum* positive sample were censored at the end of the study.

Parasite epitope types detected at each time point were the basis to re-classify episodes of *P. falciparum* infection into episodes of parasite epitope-type infection (**Figure 1**). Similar to above, we defined the beginning of each epitope episode as the first sample in which it was detected following a sample in which it was absent, and the end as the last sample in which it was detected prior to a sample in which it was absent. Censoring of infections within 14 days of a symptomatic event was performed independently of epitope types. Because most infections harbored more than one epitope, each infection episode resulted in more than one epitope-type episode.

Computing time to re-infection
Re-infection was defined as the re-appearance of any *P. falciparum* infection in a person who cleared a prior infection. A homologous re-infection was defined as the re-appearance in the same person of a parasite harboring an identical epitope type to that observed previously in that person. The time to reinfection was calculated as the interval between the end of the prior episode and the beginning of the next episode. These intervals were computed for a person's individual infection episodes, and then within these infection episodes for a person's epitope type episodes.

To determine whether our results were different from those expected by chance, we also determined time to homologous reinfection for CSP-Th2R, CSP-Th3R, and AMA-1 c1L in randomized datasets. Epitope types were randomized by permuting at the sample level within epitope MOI categories: mono-epitope (1), pauci-epitope (2-5), and multi-epitope (> 5) type episodes. This permutation scheme not only preserved the epitope type prevalences, MOI distribution, and sampling structure of the original dataset, but also maintained identical (mono) or similar (pauci- and multi-) MOIs for individual epitope-type infection episodes, reflecting a relevant null at the individual sample level and for the overall dataset. The time to homologous reinfection in the permuted dataset was then calculated as the interval between episodes with the same type as described above. Epitope types were permuted 1000x, generating 1000 randomized datasets for both CSP and AMA-1. Subsequent time-to-event analyses were performed on all permuted datasets as detailed below, and all reported measures are medians of these 1000 randomized datasets.

Hazard of reinfection
Kaplan-Meier curves were fit to estimate the proportion of individuals reinfected 1 year after an index infection. The proportional hazards assumption was assessed using Kaplan-Meier curves and plots of the log-hazard over time and, owing to the sampling scheme, only held for events with time to reinfection greater than 60 days. Thus, all subsequent analyses were performed on the subset of index infections for which time to reinfection was greater than 60 days
Mixed-effect Cox regression models were used to estimate the hazard of reinfection over the entire study period (**Equation 1**):

$$\frac{h_1(t)_i}{h_0(t)_i} = \exp(\alpha_i + \beta_1 \text{Symptomatic infection}_i + \beta_2 \text{Age 5to15}_i + \beta_3 \text{Age over 15}_i$$
$$+ \beta_4 \text{Male}_i + \beta_5 \text{Transmission intensity} + \epsilon_i)$$

These models include as covariates age (categorized as <5, 5-15, and > 15 years), sex, transmission intensity (≤ 50 or > 50 mosquitoes collected in the prior 14 days across study site), and a random intercept at the participant level (α_i) to account for repeated measures and

10

correlated outcomes within individuals. A log-normal distribution was used for the random effect. ϵ_i represents the error term of the model.

The hazard of homologous reinfection and hazard of random sub-type reinfection across participants through the entire study period was calculated using multivariate mixed effects cox regression as above with the addition of sub-type prevalence as a co-variate (**Equation 2**):

$$\frac{h_1(t)_i}{h_0(t)_i} = \exp(\alpha_i + \beta_1 \text{Symptomatic infection}_i + \beta_2 \text{Age 5 to 15}_i + \beta_3 \text{Age over 15}_i$$
$$+ \beta_4 \text{Male}_i + \beta_5 \text{Type prevalence} + \beta_6 \text{Transmission intensity} + \epsilon_i)$$

We additionally evaluated whether adding MOI as a co-variate to the multivariate mixed effects cox models influenced the hazard of homologous reinfection during the study period. In this case, MOI was defined as the number of distinct epitope types observed in the final sample of an epitope-type infection episode for a given epitope. Models including MOI as a continuous measure and as a categorical measure (1, 2-5, or >5) were evaluated and compared to the main models (Equation 2) based on model point estimates and confidence intervals (adjusted Hazard Ratios), likelihood-ratio tests, Akaike information criteria (AIC) values.

We assessed effect measure modification by epitope type prevalence by comparing the 95% confidence intervals for adjusted stratum-specific estimates and by including an interaction term between prevalence and sympomaticity in the model. The prevalence of an epitope type was defined as the proportion of all epitope-type episodes that harbored the epitope type. We used a likelihood ratio test to statistically compare model fit with and without (**Equation 2**) the interaction term.

The models for time to homologous reinfection and time to random reinfection were compared using a log-rank test. Statistical significance was assessed at an α level of 0.05. All statistical analysis and visualization were done using R (4.1.0)[33] with the packages tidyverse (1.3.1),[34] Biostrings (2.62.0),[35] ggseqlogo (0.1),[36] RandomForest(4.6-14),[37] survival (3.2-13),[38] survminer (0.4.9),[39] coxme (2.2-16),[40] ggfortify (0.4.13),[41] ggpmisc (0.4.4),[42] lubridate (1.8.0),[43] ggalt (0.4.0),[44] ggpubr (0.4.0).[45]

Data availability
Parasite sequence data are available from NCBI (PRJNA646940).

Code availability
Data and code are available on Github (https://github.com/duke-malaria-collaboratory/mozzie_epitope_analysis.git).

CONFLICT OF INTEREST
The authors have no conflicts of interest to declare.

Table 1. Comparison of symptomatic and asymptomatic index infection episodes

|	Total	Asymptomatic (n=275)	Symptomatic (n=69)	p-value*
Age, no. (%)				**0.003**
< 5y	52 (15)	43 (16)	9 (13)	
5-15	129 (38)	91 (33)	38 (55)	
> 15y	162 (47)	140 (51)	22 (32)	
Sex, no. (%)				**0.3**
Female	194 (56)	159 (58)	35 (51)	
Male	150 (44)	116 (42)	34 (49)	
Transmission season, no. (%)**				**< 0.001**
High	148 (43)	102 (37)	46 (67)	
Low	196 (57)	173 (63)	23 (33)	
Multiplicity of infection, no. (%)***				**< 0.001**
1	100 (35)	69 (31)	31 (48)	
2-5	100 (35)	74 (34)	26 (41)	
> 5	84 (30)	77 (35)	7 (11)	
Parasite density, parasites/µL, median (IQR)	**2.42 (0.47 – 62.79)**	**1.11 (0.40 – 9.62)**	**637 (50.0 – 4,770)**	**< 0.001**
Read coverage, median (IQR)				
pfcsp	6,719 (1,957 – 13,206)	4,679 (1,526 – 11,791)	12,380 (7,312 – 16,136)	< 0.001
pfama1	7,432 (3,200 – 12,939)	6,318 (2,720 – 12,014)	10,380 (7,015 – 14,880)	< 0.001

µL: microliter; *pfcsp*: *Plasmodium falciparum* circumsporozoite protein; *pfama1: P. falciparum* apical membrane antigen 1

* Computed by either the chi-square test or Wilcoxon rank sum test.

** Classified on the basis of the abundance of mosquitos collected in the prior two weeks into high (> 50) or low (≤ 50).

*** Defined as the larger of the number of unique *pfcsp* or *pfama1* nucleotide sequences in the last positive sample of an episode.
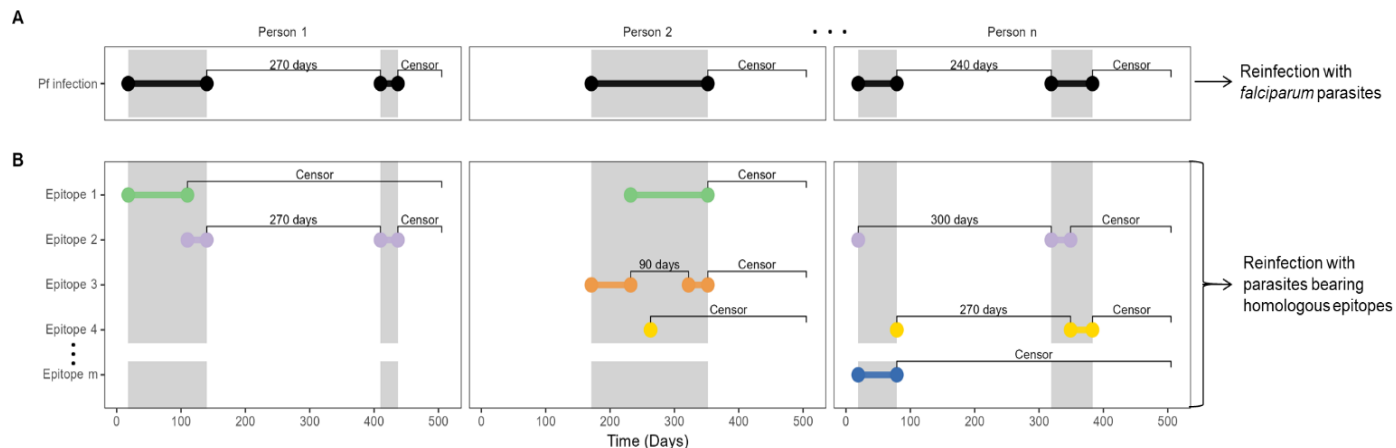
Figure 1. Calculation of time-to-reinfection based on infection episodes and on type-specific episodes. Illustration using mock data of the calculation of time-to-reinfection for 3 participants with multiple episodes. Dots indicate beginning and end of episodes, which are joined by horizontal bars. Gray shaded area indicates the time period of continuous *P. falciparum* positivity. Labels between bars indicate either time-to-reinfection (in days) or censoring following the end of an episode. (A) Pf infection indicates episodes of infection with *P. falciparum*. (B) Epitope X indicate episodes of infection with specific epitope types of *P. falciparum*, which are classified on the basis of translated nucleotide sequences of *csp* and *ama1*. Colors indicate unique CSP or AMA-1 epitopes which comprise multi-clonal infections of *P falciparum*.

14
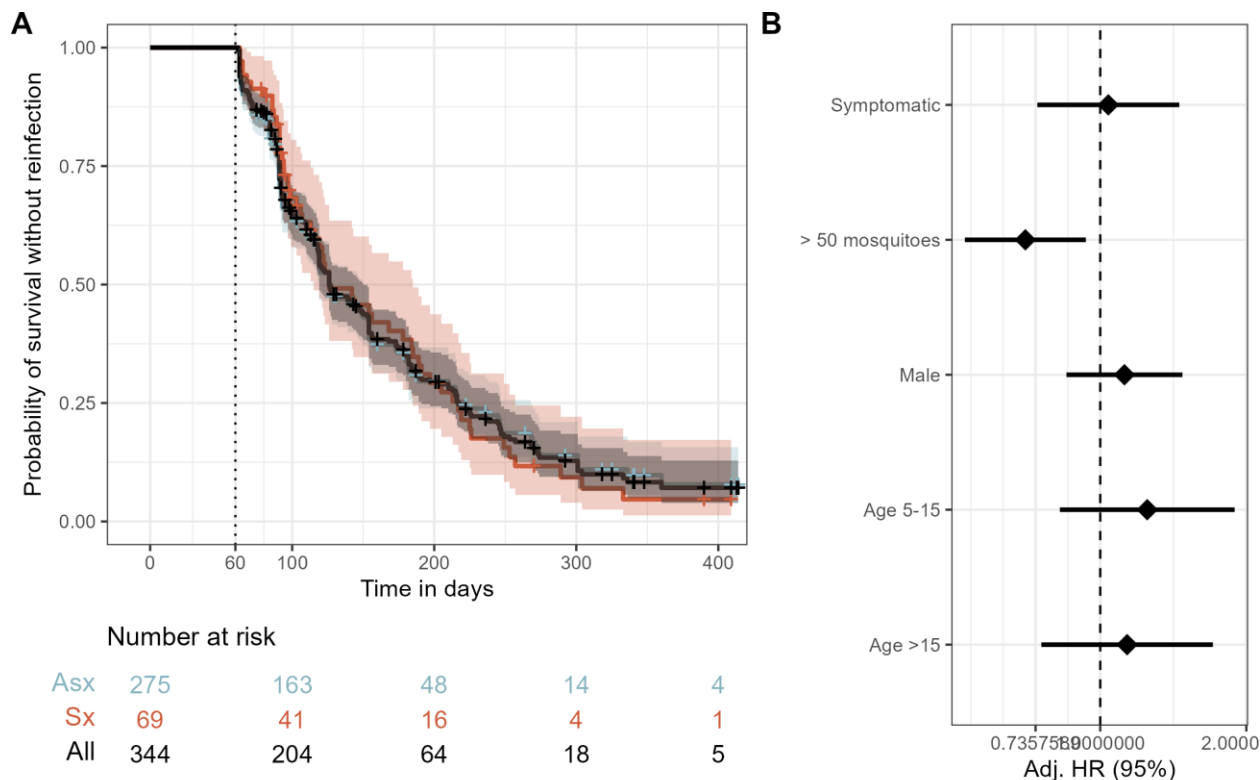
Figure 2. Risk of reinfection overall and as a function of symptomaticity of the index infection. A) Kaplan-Meier survival curve of time to reinfection with *P. falciparum*. The black line is the probability among all participants, and colored lines are probability stratified by index case as either asymptomatic (Asx, blue) or symptomatic (Sx, red). Note that the blue line is largely hidden by the black line. Crosses indicate infections that were not followed by a reinfection and therefore censored at the end of the study period. Vertical dotted line indicates the start of the defined time at risk of re-infection, shaded areas indicate the 95% confidence interval, and table shows the number of participants at risk stratified by symptomaticity of index infection at day 0, 100, 200, 300, and 400. **B)** Adjusted Hazard Ratios for reinfection estimated by a multivariate mixed effects Cox proportional hazards model. Diamonds indicate adjusted HRs, and bars show the 95% CIs. Adj. HR: Adjusted Hazard Ratio
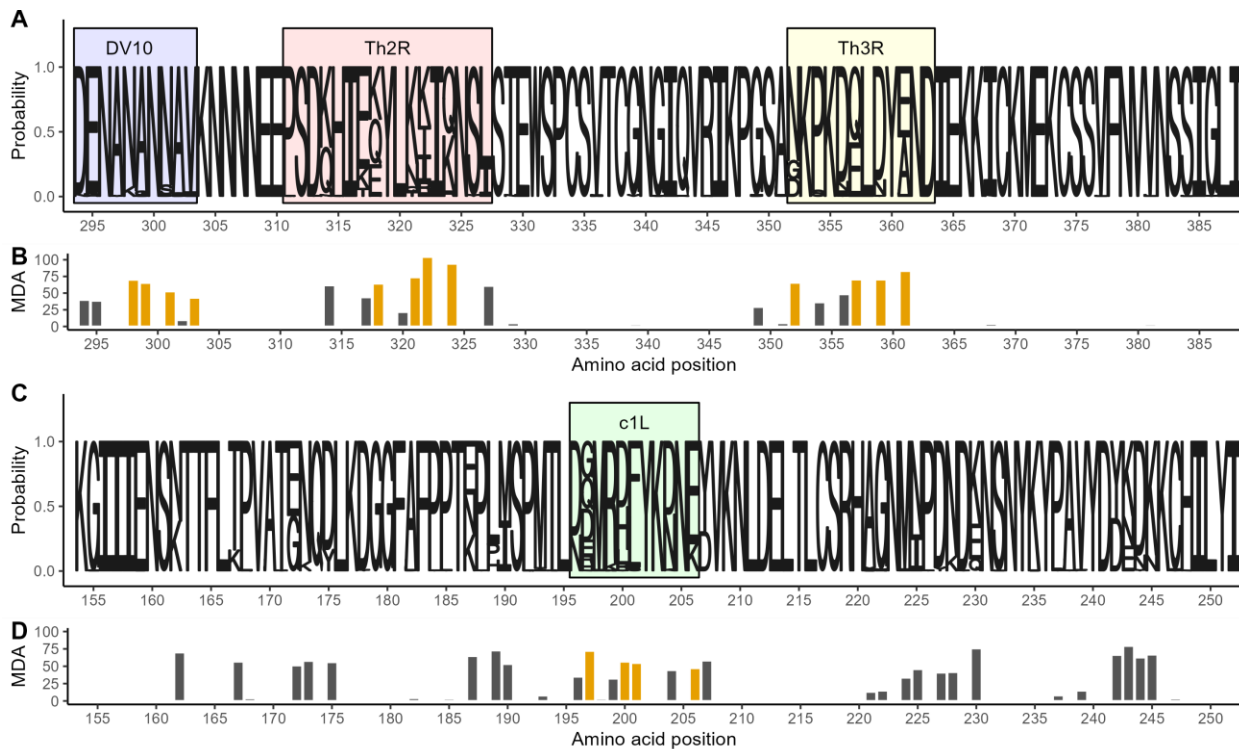
Figure 3. Amino acid diversity of sequenced *pfcsp* and *ama1* fragments. A) Sequence logo of the observed circumsporozoite protein (CSP) amino acid variation. The size of the letters at each position shows the probability of the specific residue. Boxes indicate the positions of known epitopes for B-cells (DV10, blue), CD4+ T-cells (Th2R, red) and CD8+ T-cells (Th3R, yellow). **B)** Result of a random forest model used to predict the whole CSP fragment nucleotide sequence using amino acid variation. Bar height indicates for each variant amino acid position the mean decrease in accuracy (MDA) of prediction. Gold indicates the four most predictive amino acid positions within each T-cell epitope. **C)** Sequence logo of the observed apical membrane antigen 1 (AMA-1) amino acid variation. The size of the letters at each position shows the probability of the specific residue. Green box marks the c1L domain. **D)** The mean decrease in accuracy for each variant amino acid position in a random forest model used to predict the whole AMA-1 fragment nucleotide sequence. Gold indicates the four most predictive amino acid positions within the c1L domain.

16
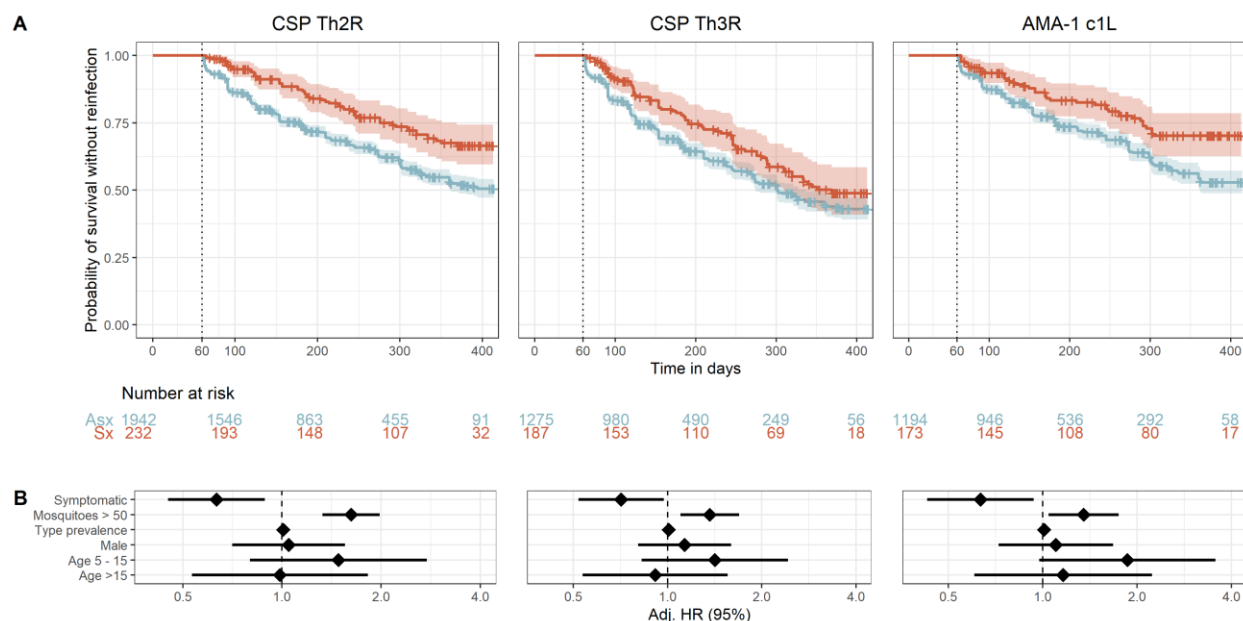
Figure 4. Time to reinfection by homologous *P. falciparum* parasites stratified by symptomaticity of index infection. A) Kaplan-Meier survival curves of time to reinfection by parasites with homologous CSP-Th2R, CSP-Th3R, and AMA-1 c1L type. Curves are probability stratified by index case as either asymptomatic (Asx, blue) or symptomatic (Sx, red). Crosses indicate index infections that were censored at the end of the study period. Vertical dotted line indicates the start of the defined time at risk of re-infection, shaded areas indicate the 95% confidence interval, and table shows the number of participants at risk stratified by symptomaticity of index infection at day 0, 100, 200, 300, and 400. **B)** Adjusted Hazard Ratios estimated by multivariate mixed effects Cox proportional hazards models for reinfection by parasites bearing homologous CSP-Th2R, CSP-Th3R, and AMA-1 c1L epitope types. Diamonds indicate adjusted HRs, and bars show the 95% CIs. Adj. HR, Adjusted Hazard Ratio.
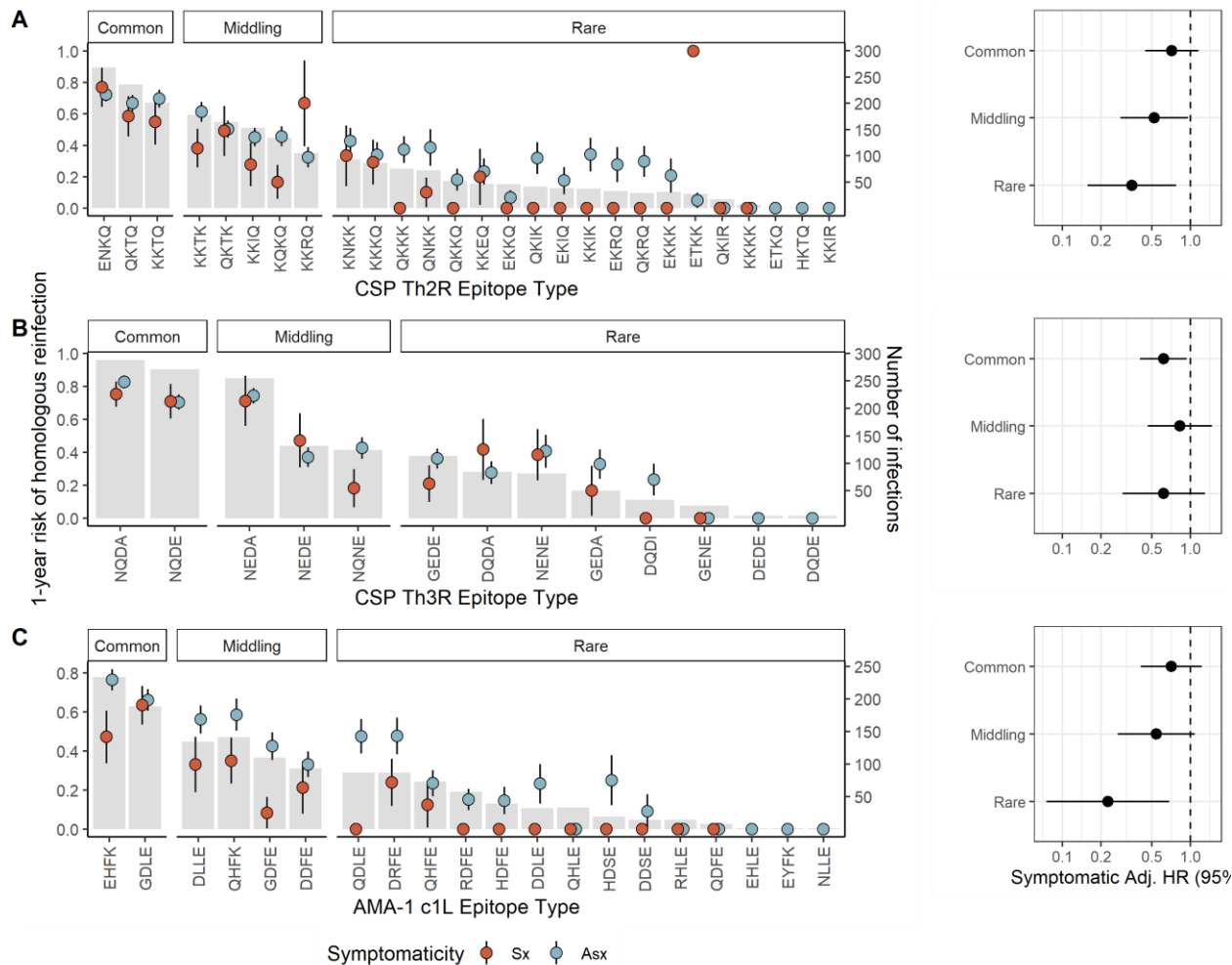
Figure 5. **Prevalence of epitope types and time to homologous reinfection following asymptomatic and symptomatic infections. Left:** Gray bars indicate the number of infections harboring each CSP-Th2R **(A)**, CSP-Th3R **(B)**, or AMA-1 c1L **(C)** epitope type (right y-axis). Dots indicate the proportion of each index infection harboring the epitope type that was followed by homologous reinfection after 1 year (left y-axis) for either symptomatic (red) or asymptomatic (blue) index infections, with lines as standard error. **Right**: Adjusted Hazard Ratios for symptomatic index infections estimated by multivariate mixed effects Cox proportional hazards models for reinfection by parasites bearing homologous CSP-Th2R epitopes (A), CSP-Th3R (B), or AMA-1 c1L (C) epitopes that are individually classified as common, middling, and rare, as indicated in the bar plot. Hazard ratios adjusted for age, epitope type prevalence, gender, and transmission season. Circles indicate adjusted HRs, and bars show the 95% CIs. Adj. HR, Adjusted Hazard Ratio.

18

REFERENCES

1   WHO. *World Malaria Report 2018*, <https://www.who.int/malaria/publications/world-malaria-report-2018/en/> (2018).

2   Gupta, S., Snow, R. W., Donnelly, C. A., Marsh, K. & Newbold, C. Immunity to non-cerebral severe malaria is acquired after one or two infections. *Nature medicine* **5**, 340-343, doi:10.1038/6560 (1999).

3   Coley, A. M. *et al.* The most polymorphic residue on Plasmodium falciparum apical membrane antigen 1 determines binding of an invasion-inhibitory antibody. *Infection and immunity* **74**, 2628-2636, doi:10.1128/IAI.74.5.2628-2636.2006 (2006).

4   Healer, J. *et al.* Allelic polymorphisms in apical membrane antigen-1 are responsible for evasion of antibody-mediated inhibition in Plasmodium falciparum. *Molecular microbiology* **52**, 159-168, doi:10.1111/j.1365-2958.2003.03974.x (2004).

5   Hodder, A. N., Crewther, P. E. & Anders, R. F. Specificity of the protective antibody response to apical membrane antigen 1. *Infection and immunity* **69**, 3286-3294, doi:10.1128/IAI.69.5.3286-3294.2001 (2001).

6   Kennedy, M. C. *et al.* In vitro studies with recombinant Plasmodium falciparum apical membrane antigen 1 (AMA1): production and activity of an AMA1 vaccine and generation of a multiallelic response. *Infection and immunity* **70**, 6948-6960, doi:10.1128/IAI.70.12.6948-6960.2002 (2002).

7   Neafsey, D. E. *et al.* Genetic Diversity and Protective Efficacy of the RTS,S/AS01 Malaria Vaccine. *The New England journal of medicine* **373**, 2025-2037, doi:10.1056/NEJMoa1505819 (2015).

8   Doolan, D. L., Dobano, C. & Baird, J. K. Acquired immunity to malaria. *Clinical microbiology reviews* **22**, 13-36, Table of Contents, doi:10.1128/CMR.00025-08 (2009).

9   Seder, R. A. *et al.* Protection against malaria by intravenous immunization with a nonreplicating sporozoite vaccine. *Science* **341**, 1359-1365, doi:10.1126/science.1241800 (2013).

10   Epstein, J. E. *et al.* Protection against Plasmodium falciparum malaria by PfSPZ Vaccine. *JCI Insight* **2**, e89154, doi:10.1172/jci.insight.89154 (2017).

11   Collins, W. E., Jeffery, G. M. & Roberts, J. M. A retrospective examination of reinfection of humans with Plasmodium vivax. *The American journal of tropical medicine and hygiene* **70**, 642-644 (2004).

12   Ouattara, A. *et al.* Epitope-based sieve analysis of Plasmodium falciparum sequences from a FMP2.1/AS02A vaccine trial is consistent with differential vaccine efficacy against immunologically relevant AMA1 variants. *Vaccine* **38**, 5700-5706, doi:10.1016/j.vaccine.2020.06.035 (2020).

13   Sumner, K. M. *et al.* Genotyping cognate Plasmodium falciparum in humans and mosquitoes to estimate onward transmission of asymptomatic infections. *Nature communications* **12**, 909, doi:10.1038/s41467-021-21269-2 (2021).

14   Tran, T. M. *et al.* Transcriptomic evidence for modulation of host inflammatory responses during febrile Plasmodium falciparum malaria. *Scientific reports* **6**, 31291, doi:10.1038/srep31291 (2016).

15   Portugal, S. *et al.* Exposure-dependent control of malaria-induced inflammation in children. *PLoS pathogens* **10**, e1004079, doi:10.1371/journal.ppat.1004079 (2014).

16   Long, Q. X. *et al.* Clinical and immunological assessment of asymptomatic SARS-CoV-2 infections. *Nature medicine* **26**, 1200-1204, doi:10.1038/s41591-020-0965-6 (2020).

17   Guttinger, M. *et al.* Human T cells recognize polymorphic and non-polymorphic regions of the Plasmodium falciparum circumsporozoite protein. *The EMBO journal* **7**, 2555-2558, doi:10.1002/j.1460-2075.1988.tb03104.x (1988).

18   Kumar, S. *et al.* Cytotoxic T cells specific for the circumsporozoite protein of Plasmodium falciparum. *Nature* **334**, 258-260, doi:10.1038/334258a0 (1988).

19   Dutta, S., Lee, S. Y., Batchelor, A. H. & Lanar, D. E. Structural basis of antigenic escape of a malaria vaccine candidate. *Proceedings of the National Academy of Sciences of the United States of America* **104**, 12488-12493, doi:10.1073/pnas.0701464104 (2007).

20   Kurup, S. P., Butler, N. S. & Harty, J. T. T cell-mediated immunity to malaria. *Nat Rev Immunol* **19**, 457-471, doi:10.1038/s41577-019-0158-z (2019).

21   Romero, P. *et al.* Cloned cytotoxic T cells recognize an epitope in the circumsporozoite protein and protect against malaria. *Nature* **341**, 323-326, doi:10.1038/341323a0 (1989).

22   Reece, W. H. *et al.* A CD4(+) T-cell immune response to a conserved epitope in the circumsporozoite protein correlates with protection from natural Plasmodium falciparum infection and disease. *Nature medicine* **10**, 406-410, doi:10.1038/nm1009 (2004).

23   Takala, S. L. *et al.* Extreme polymorphism in a vaccine antigen and risk of clinical malaria: implications for vaccine development. *Science translational medicine* **1**, 2ra5, doi:10.1126/scitranslmed.3000257 (2009).

24   Cortes, A. *et al.* Allele specificity of naturally acquired antibody responses against Plasmodium falciparum apical membrane antigen 1. *Infection and immunity* **73**, 422-430, doi:10.1128/IAI.73.1.422-430.2005 (2005).

25   Baer, K., Klotz, C., Kappe, S. H., Schnieder, T. & Frevert, U. Release of hepatic Plasmodium yoelii merozoites into the pulmonary microvasculature. *PLoS pathogens* **3**, e171, doi:10.1371/journal.ppat.0030171 (2007).

26   Cockburn, I. A., Tse, S. W. & Zavala, F. CD8+ T cells eliminate liver-stage Plasmodium berghei parasites without detectable bystander effect. *Infection and immunity* **82**, 1460-1464, doi:10.1128/IAI.01500-13 (2014).

27   McNamara, H. A. *et al.* Up-regulation of LFA-1 allows liver-resident memory T cells to patrol and remain in the hepatic sinusoids. *Sci Immunol* **2**, doi:10.1126/sciimmunol.aaj1996 (2017).

28   Cui, W. & Kaech, S. M. Generation of effector CD8+ T cells and their conversion to memory T cells. *Immunological reviews* **236**, 151-166, doi:10.1111/j.1600-065X.2010.00926.x (2010).

29   Finney, O. C., Riley, E. M. & Walther, M. Regulatory T cells in malaria--friend or foe? *Trends in immunology* **31**, 63-70, doi:10.1016/j.it.2009.12.002 (2010).

30   O'Meara, W. P. *et al.* Mosquito Exposure and Malaria Morbidity: A Microlevel Analysis of Household Mosquito Populations and Malaria in a Population-Based Longitudinal Cohort in Western Kenya. *The Journal of infectious diseases* **221**, 1176-1184, doi:10.1093/infdis/jiz561 (2020).

31   Sumner, K. M. *et al.* Exposure to Diverse Plasmodium falciparum Genotypes Shapes the Risk of Symptomatic Malaria in Incident and Persistent Infections: A Longitudinal Molecular Epidemiologic Study in Kenya. *Clinical infectious diseases : an official publication of the Infectious Diseases Society of America* **73**, 1176-1184, doi:10.1093/cid/ciab357 (2021).

32   Taylor, S. M. *et al.* Direct Estimation of Sensitivity of Plasmodium falciparum Rapid Diagnostic Test for Active Case Detection in a High-Transmission Community Setting. *The American journal of tropical medicine and hygiene* **101**, 1416-1423, doi:10.4269/ajtmh.19-0558 (2019).

33   R: A language and environment for statistical computing (R Foundation for Statistical Computing, Vienna, Austria, 2021).

34   Wickham, H. *et al.* Welcome to the Tidyverse. *Journal of open source software* **4**, 1686 (2019).

35   Biostrings: Efficient manipulations of biological strings. R package version 2.62.0 (2021).

36   ggseqlogo: A 'ggplot2' Estension fro Drawing Publication-Ready Sequence Logos. R package version 0.1 (2017).

37   Liaw, A. & Wiener, M. C.

38   Therneau, T. & Grambsch, P. *Modeling Survival Data: Extending the Cox Model*. 1 edn, (Springer, 2000).
39   survminer: Drawing Survival Curves using 'ggplot2.' R package version 0.4.9 (2021).
40   coxme: Mixed Effects Cox Models. R package version 2.2-16. (2020).
41   ggfortify: Unified Interface to Visualize Statistical Results of Popular R Packages (2016).
42   ggpmisc: Miscellaneous Extensions to 'ggplot2.' R package version 0.4.4. (2021).
43   Grolemund, G. & Wickham, H. Dates and Times Made Easy with lubridate. *Journal of Statistical Software* **40**, 1 - 25, doi:10.18637/jss.v040.i03 (2011).
44   ggalt: Extra Coordinate Systems, 'Geoms,' Statistical Transformations, Scales, and Fonts for 'ggplot2.' R package version 0.4.0 (2017).
45   ggpubr: 'ggplot2' Based Publication Ready Plots. R package version 0.4.0 (2020).

Supplemental Results

Analysis of CSP DV10 positions
When classified by CSP-DV10 epitope type, we observed 897 type infection episodes. The probability of homologous CSP-DV10 epitope type reinfection within 1 year was 0.71 (95% CI 0.67 – 0.75), similar to reinfection with a random epitope type (log-rank median chisq 0.661, p = 0.416) (**Supplemental Figure 5A**). In randomized datasets, there was no difference in the risk of homologous reinfection between symptomatic and asymptomatic infections (**Supplemental Figure 5B**; log-rank test median chisq 0.425, p = 0.514). There was not a statistically significant decrease in the hazard of reinfection with parasites bearing homologous CSP-DV10 epitope types following symptomatic compared to asymptomatic index episodes; however, the estimated adjusted hazard ratio (aHR 0.75, 95% CI 0.53 – 1.05, p = 0.098) followed similar trends to the CSP-Th2R, CSP-Th3R, and AMA-1 c1L epitopes (**Supplemental Figure 5C**).

Ensemble analysis of CSP Th2R and Th3R positions
We re-classified parasites on the basis of the 4 most informative amino acid positions in each of the CSP-Th2R and the -Th3R epitopes (**Figure 3)** yielding 84 unique CSP-Th2R/Th3R types. As with prior classifications using only either epitope, the MOI expressed by these epitopes was highly correlated with the *pfcsp* nucleotide sequence (**Supplemental Figure 6A**). The probability of homologous CSP Th2R/Th3R epitope type reinfection within 1 year was 0.41 (95% CI 0.38 – 0.44), which was similar to reinfection with a heterologous parasite in randomized datasets (log-rank median chisq 1.53, p=0.217) (**Supplemental Figure 6D**), in which there was no difference in the hazard of homologous reinfection between symptomatic and asymptomatic infections (median aHR 1.02; 95% CI 0.79 – 1.32) (**Supplemental Figure 6C**). However, similar to the associations observed for parasites defined on either CSP Th receptor epitope, compared to asymptomatic index infections, the hazard of reinfection with parasites bearing a homologous CSP Th2R/Th3R epitope type following a symptomatic infection was decreased by 44% (aHR 0.56; 95% CI 0.40 – 0.80; p=0.002) (**Supplemental Figure 6B**).

Supplemental Table 1. **Comparison of index infection episodes included and excluded from survival analyses**

	Total	Included	Excluded	p-value*
Time to censoring, mean, days	99.94	137.56	37.43	2.2e-16
Type, no. (%)				
Asymptomatic	415 (75.3)	275 (79.9)	140 (67.6)	0.0012
Symptomatic	136 (24.7)	69 (20.1)	67 (32.4)	
Age, no. (%)				
< 5y	84 (15.3)	52 (15.2)	32 (15.6)	
5-15	228 (41.6)	129 (37.6)	99 (48.3)	0.0270
>15y	236 (43.1)	162 (47.2)	74 (36.1)	
Sex, no. (%)				
Female	315 (57.2)	194 (56.4)	121 (58.5)	0.636
Male	236 (42.8)	150 (43.6)	86 (41.5)	
Transmission season, no. (%) **				
High	268 (48.6)	148 (43.0)	120 (58.0)	0.001
Low	283 (51.4)	196 (57.0)	87 (42.0)	

Infections were excluded from survival analyses if reinfection occurred ≤ 60d following the end of the index infection.
* Computed by either the chi-square test or t-test.
** Classified on the basis of the abundance of mosquitos collected in the prior two weeks into high (> 50) or low (≤ 50).

Supplemental Table 2. Cox mixed effect model estimates for reinfection with parasites bearing homologous epitope types after symptomatic and asymptomatic exposure, without and with adjustment for MOI.

	Main model (no MOI) Adj. HR (95% CI)	Model with continuous MOI Adj. HR (95% CI)	Model with categorical MOI Adj. HR (95% CI)
Epitope			
CSP Th2R			
Symptomatic infection	**0.63 (0.45 – 0.89)**	**0.60 (0.45 – 0.84)**	**0.61 (0.43 – 0.85)**
Mosquitoes > 50	1.62 (1.33 – 1.98)	1.61 (1.31 – 1.96)	1.62 (1.33 – 1.98)
Type prevalence	1.22 (1.19 – 1.25)	1.22 (1.19 – 1.25)	1.22 (1.19 – 1.25)
Male	1.05 (0.71 – 1.55)	1.05 (0.71 – 1.55)	1.04 (0.70 – 1.53)
Age 5-15	1.48 (0.80 – 2.76)	1.45 (0.78 – 2.69)	1.46 (0.79 – 2.69)
Age > 15	0.99 (0.53 – 1.82)	0.97 (0.52 – 1.79)	0.98 (0.53 – 1.80)
MOI (continuous)	---	0.97 (0.95 – 1.00)	---
MOI 2-5	---	---	1.20 (0.86 – 1.67)
MOI > 5	---	---	0.91 (0.64 – 1.28)
AIC	611.00	612.15	611.76
LR test, p-value*		0.1263	0.0676
CSP Th3R			
Symptomatic infection	**0.71 (0.52 – 0.97)**	**0.68 (0.49 – 0.93)**	**0.71 (0.52 – 0.97)**
Mosquitoes > 50	1.36 (1.10 – 1.69)	1.36 (1.10 – 1.68)	1.36 (1.10 – 1.69)
Type prevalence	1.13 (1.11 – 1.14)	1.12 (1.11 – 1.14)	1.13 (1.11 – 1.14)
Male	1.13 (0.80 – 1.60)	1.14 (0.81 – 1.61)	1.13 (0.81 – 1.60)
Age 5-15	1.42 (0.83 – 2.42)	1.39 (0.81 – 2.38)	1.40 (0.82 – 2.40)
Age > 15	0.91 (0.54 – 1.56)	0.90 (0.52 – 1.53)	0.91 (0.54 – 1.55)
MOI (continuous)	---	0.96 (0.90 – 1.01)	---
MOI 2-5	---	---	1.01 (0.76 – 1.35)
MOI > 5	---	---	0.93 (0.65 – 1.33)
AIC	411.60	412.99	407.98
LR test, p-value*		0.1934	0.8630
AMA-1 c1L			
Symptomatic infection	**0.63 (0.43 – 0.94)**	**0.54 (0.37 – 0.81)**	**0.56 (0.37 – 0.84)**
Mosquitoes > 50	1.35 (1.04 – 1.75)	1.36 (1.06 – 1.76)	1.40 (1.08 – 1.81)
Type prevalence	1.16 (1.13 – 1.18)	1.15 (1.13 – 1.18)	1.16 (1.13 – 1.18)
Male	1.10 (0.72 – 1.69)	1.06 (0.69 – 1.64)	1.01 (0.65 – 1.59)
Age 5-15	1.86 (0.96 – 3.56)	1.77 (0.91 – 3.44)	1.78 (0.90 – 3.53)
Age > 15	1.16 (0.60 – 2.23)	1.14 (0.58 – 2.22)	1.15 (0.58 – 2.30)
MOI (continuous)	---	0.92 (0.87 – 0.97)	---
MOI 2-5	---	---	1.40 (0.97 – 1.97)
MOI > 5	---	---	0.74 (0.50 – 1.10)
AIC	355.66	368.29	377.64
LR test, p-value*		0.0028	0.0003

* Relative to "Main model (no MOI)"

AIC: Akaike information criterion; LR: likelihood ratio
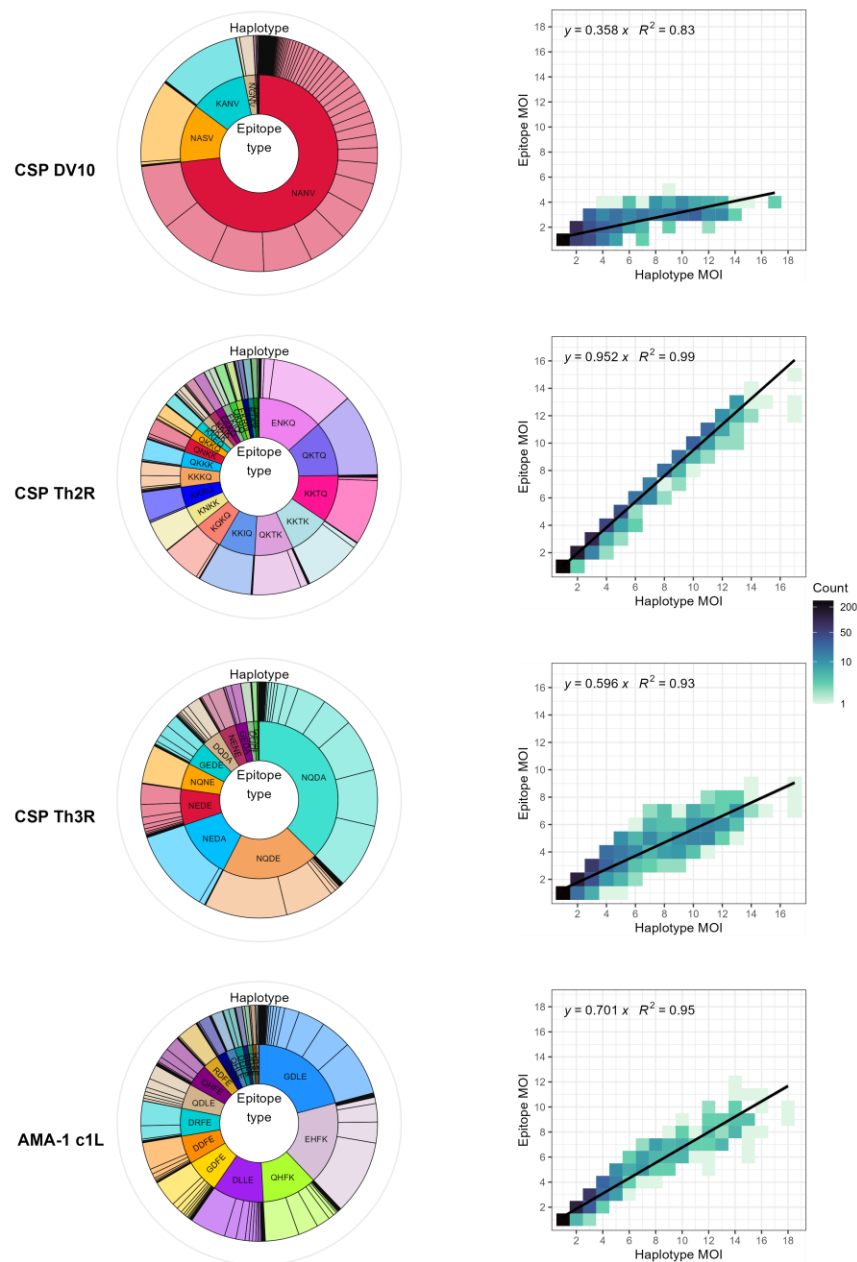
Supplemental Figure 1. Comparative diversity of nucleotide haplotypes and epitope types. Left: Sunburst plots displaying haplotypes (outer circle) defined on unique nucleotide sequences of each fragment and corresponding epitope types (inner circle) for each protein fragment defined by the four most important amino acid positions observed in the CSP DV10 epitope (amino acid positions 298, 299, 301, 303, n = 861 samples), CSP-Th2R epitope (amino acid positions 318, 321, 322, 324, n = 861 samples), CSP-Th3R epitope (amino acid positions 352, 357, 359, 361, n = 861 samples), and AMA-1 c1L (amino acid positions 197, 200, 201, 206, n = 724 samples). Right: Plots of the correlation between multiplicity of infection (MOI) defined by nucleotide haplotype and by epitope type defined by the four most important amino acid positions observed in the CSP DV10 epitope, CSP Th2R epitope, CSP Th3R epitope, and AMA-1 c1L domain. Color indicates the number of samples within each bin, and lines are regression output.

25
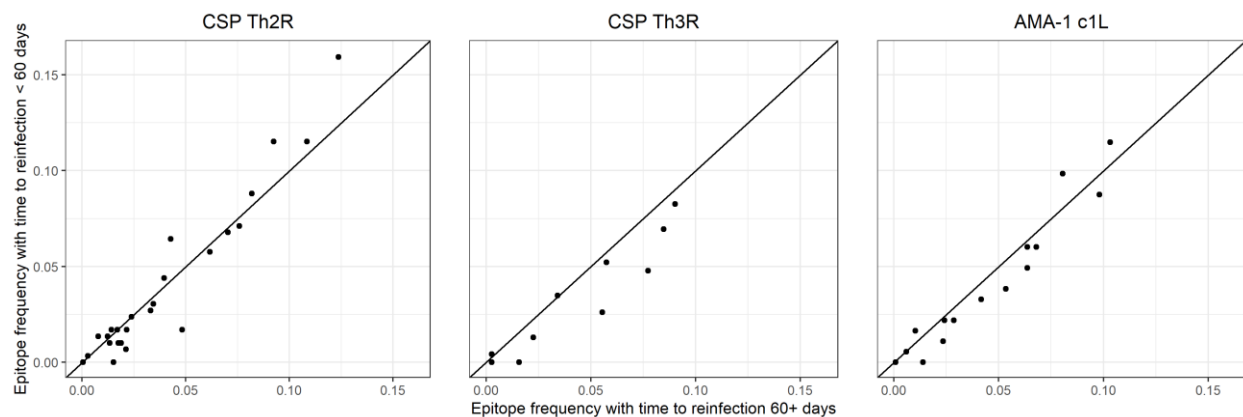
Supplemental Figure 2. Comparison of epitope type frequencies in index infections with time to reinfection less than or greater than 60 days. Each dot indicates the prevalence of a unique CSP-Th2R (left), CSP-Th3R (middle), or AMA-1 c1L (right) type in index infections with (y-axis) or without (x-axis) reinfection within the first 60 days following clearance. Black line indicates X=Y.
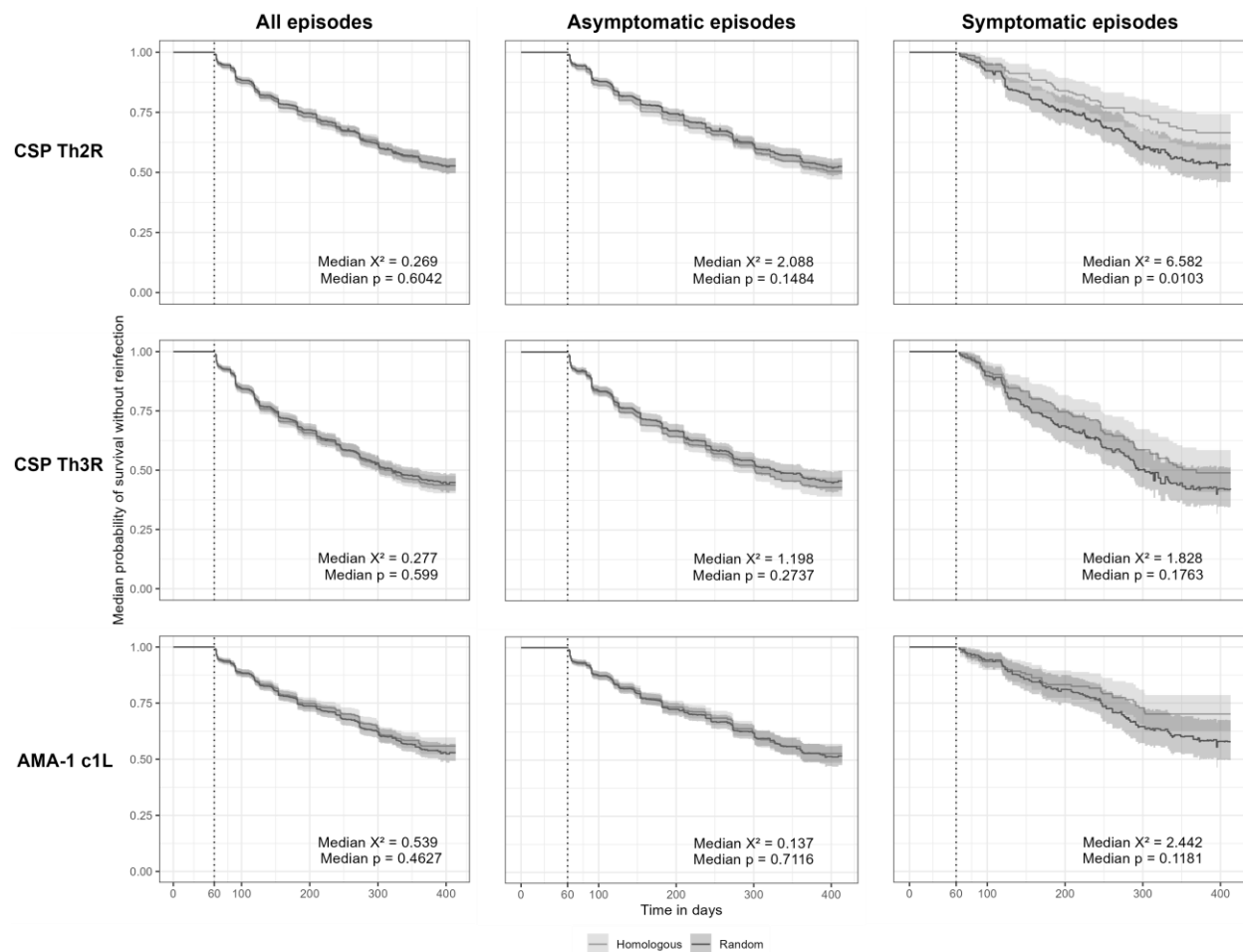
Supplemental Figure 3. Risk of reinfection with *P. falciparum* parasites bearing homologous epitopes. Kaplan-Meier survival curves of time to homologous type reinfection defined by the CSP-Th2R epitope (top), CSP-Th3R epitope (middle), or the AMA-1 c1L epitope type (bottom) stratified on the observed dataset (grey) or randomized datasets (black) after all index episodes (left), asymptomatic index episodes (middle) and symptomatic index episodes (right). Each unique type present in a sample was considered an index case when the type was absent in the subsequent sample. Reinfection was defined as first sample harboring the same specific type. Time to reinfection with a random type was determined by permuting epitope types at the sample level and then treated as the time to homologous reinfection. Survival curves for reinfection with random epitopes represent the median survival probabilities and confidence intervals of 1000 permuted datasets. Infections that were not followed by a reinfection were censored at the end of the study period and are denoted by crosses. Vertical dotted line indicates the start of the defined time at risk of re-infection, and shaded area shows the 95% CIs.
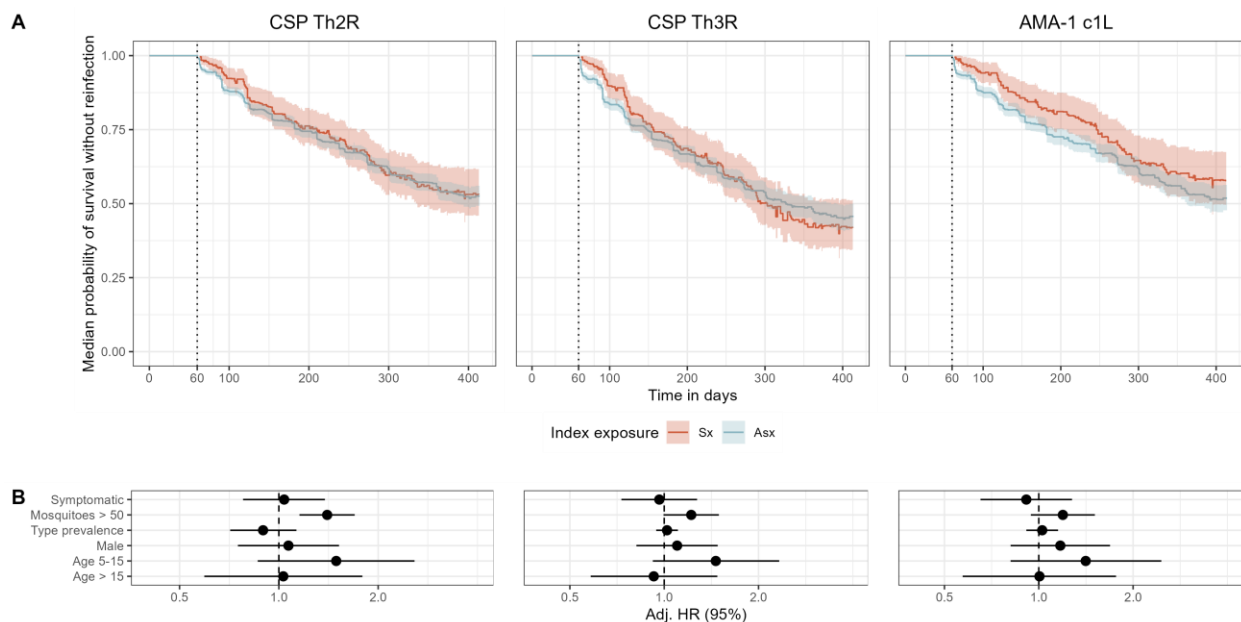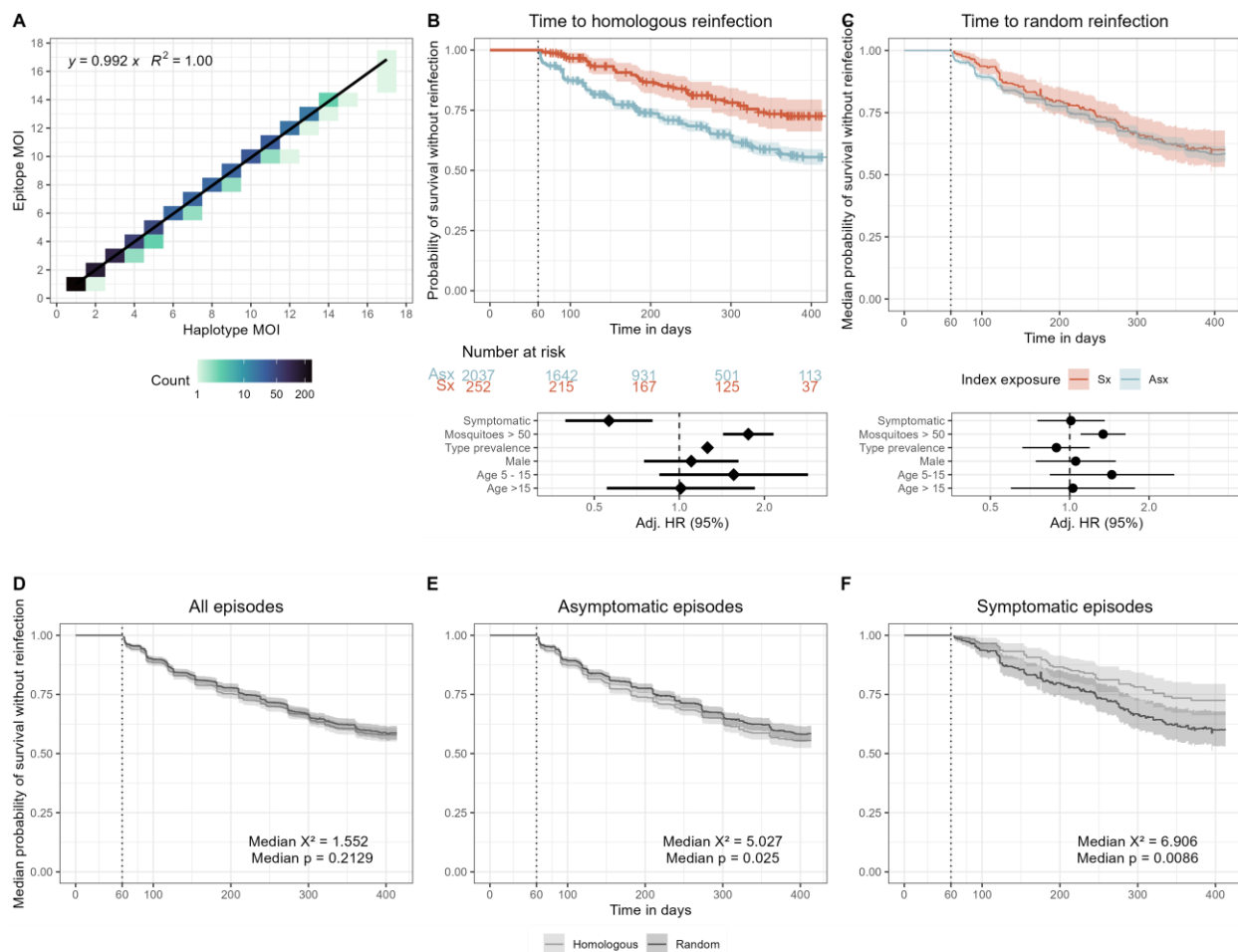
Supplemental Figure 4. Time to reinfection with random epitope type stratified by symptomaticity. A) Kaplan-Meier survival curves of time to reinfection by parasites with random CSP-Th2R type, CSP-Th3R type, or AMA-1 c1L types. Randomized datasets (1000) were generated by permuting epitope types at the sample level, and median survival probabilities are plotted. For each infection and each antigen, each unique type is treated as a separate unique infection. Curves are stratified by index case being either asymptomatic (Asx) or symptomatic (Sx). Infections that were not followed by a reinfection were censored at the end of the study period. Shaded areas indicate the median 95% confidence interval (CI). **B)** Median mixed effects Cox proportional hazards model results for reinfection with homologous CSP Th2R epitope types, homologous CSP Th3R epitope types, and homologous AMA-1 c1L types. Circles indicate the median adjusted Hazard Ratio (HR); lines show the median 95% confidence interval. Adj. HR, adjusted hazard ratio.
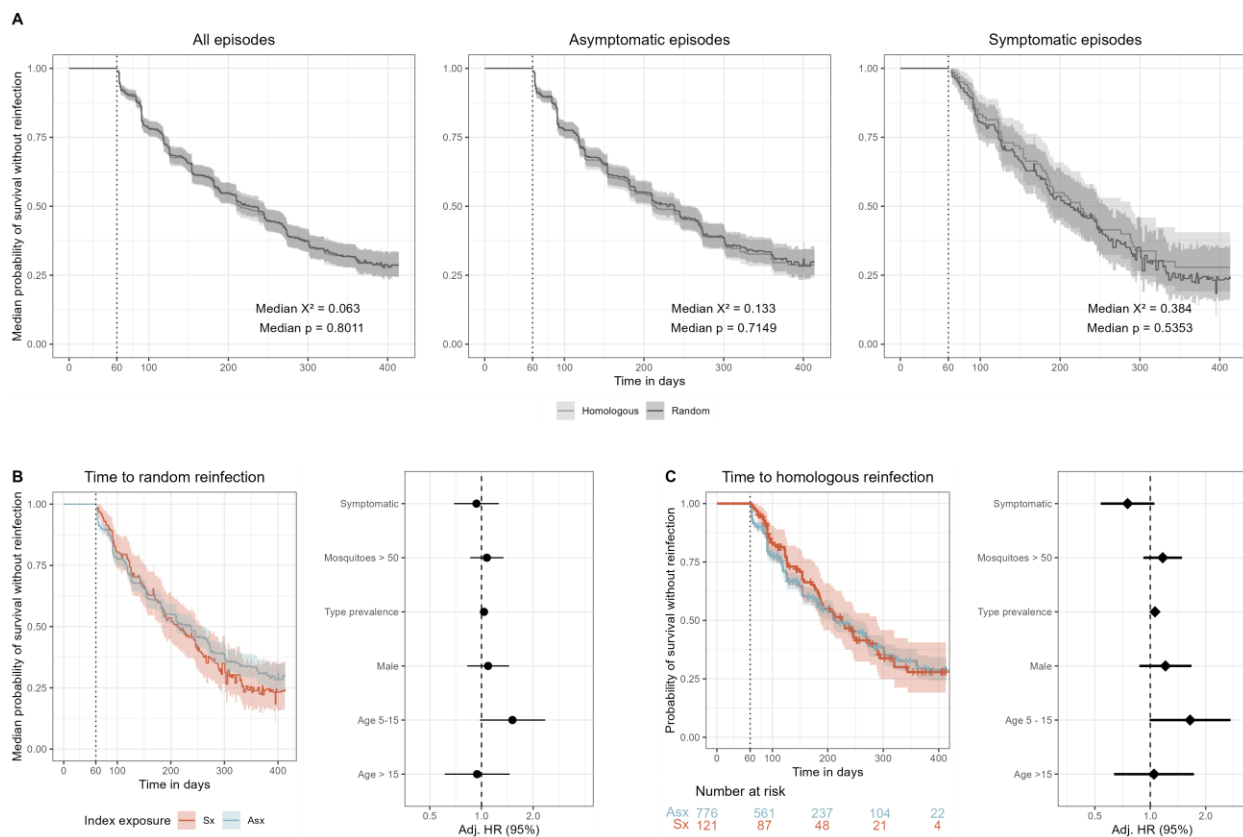
Supplemental Figure 5. Analyses of parasites defined by CSP DV10. A) Kaplan-Meier survival curves of time to homologous type reinfection defined by the CSP-DV10 epitope stratified on the observed dataset (grey) or randomized datasets (black) after all index episodes (left), asymptomatic index episodes (middle) and symptomatic index episodes (right). **B)** Kaplan-Meier survival curves of time to reinfection by parasites with random CSP-DV10 types after asymptomatic index episodes (blue) and symptomatic epidodes (red) and median mixed effects Cox proportional hazards model results for reinfection with random CSP-DV10 epitope types. Circles indicate the median adjusted Hazard Ratio (HR). **C)** Kaplan-Meier survival curves of time to reinfection by parasites with homologous CSP-DV10 types after asymptomatic index episodes (blue) and symptomatic epidodes (red) and mixed effects Cox proportional hazards model results for reinfection with homologous CSP-DV10 epitope types. Diamonds indiciate adjusted Hazard Ratio (HR); lines show the median 95% confidence interval. Adj. HR, adjusted hazard ratio.

Supplemental Figure 6. Analyses of parasites defined by combined CSP-Th2R/Th3R epitopes. A) Plot of the correlation between multiplicity of infection (MOI) defined by nucleotide haplotype and by epitope type defined by the 8 most important amino acid positions observed in the combined CSP-Th2R/Th3R epitope. Color indicates the number of samples within each bin, and lines are regression output. **B) and C)** Kaplan-Meier survival curves of time to reinfection by parasites with homologous combined CSP-Th2R/Th3R type **(B)** or random combined CSP-Th2R/Th3R type **(C).** Curves are probability stratified by index case as either asymptomatic (Asx, blue) or symptomatic (Sx, red). Table shows the number of participants at risk stratified by symptomaticity of index infection at day 0, 100, 200, 300, and 400. For **(C)**, Randomized datasets (1000) were generated by permuting epitope types at the sample level, and median survival probabilities are plotted. Adjusted Hazard Ratios estimated by multivariate mixed effects Cox proportional hazards models for reinfection by parasites bearing homologous CSP-Th2R/Th3R epitopes **(B)** or random CSP-Th2R/Th3R epitopes **(C).** For survival curves, crosses indicate infections that were not followed by a reinfection with a homologous parasite type and therefore censored at the end of the study period, vertical dotted line indicates the start of the defined time at risk of re-infection, and shaded areas indicate the 95% confidence interval. Diamonds indicate adjusted HRs, and bars show the 95% CIs. Adj. HR, adjusted hazard ratio. **D), E), F)** Kaplan-Meier survival curve of time to homologous type reinfection defined by the CSP-Th2R/Th3R epitope stratified on the observed dataset (grey) or randomized datasets (black) after all index episodes **(D)**, asymptomatic index episodes **(E)**, and symptomatic episodes **(F)**. Time to reinfection with a random type was determined by permuting epitope types at the sample level and then treated as the time to homologous reinfection. Survival

30

curves for reinfection with random epitopes represent the median survival probabilities and confidence intervals of 1000 permuted datasets. Crosses indicate infections that were not followed by a reinfection with a homologous parasite type and therefore censored at the end of the study period. Vertical dotted line indicates the start of the defined time at risk of re-infection, shaded areas indicate the 95% confidence interval.